Int. J. Solids Structures Vol. 30, No. 10, pp. 1369–1378, 1993
Printed in Great Britain

0020-7683/93 $6.00+ .00

BENDING STRESS ENHANCEMENT IN MATERIALS WITH LIMITED SHEAR RESISTANCE—PART II. UNLAYERED SHEAR-WEAK MODEL

P. S. STEIF and A. TROJNACKI
Department of Mechanical Engineering, Carnegie Mellon University, Pittsburgh, PA 15213, U.S.A.

(*Received* 30 *December* 1991; *in revised form* 4 *November* 1992)

Abstract—An alternative model for materials with limited shear resistance is explored. Quantitative comparisons with the layered-beam considered in Part I are presented. Finally, we draw some conclusions regarding composite strength in bending.

1. INTRODUCTION

The purpose of this two-part paper is to gain insight into the bending stress enhancement which can develop in fiber composites due to limited shear resistance. One model for a material with limited shear resistance was presented in Part I. We considered a beam consisting of a number of discrete layers; these layers can slip with respect to one another when the shear stress reaches a critical value. A general approach to analysing such beams was developed, based primarily on the assumption that each layer can be treated using the usual beam-theory approximations. The method was used to analyse a layered beam in three-point bending, which revealed some aspects of bending stress enhancement.

Unfortunately, analysing layered beams is computationally intensive, even for the simplest loadings. Moreover, modeling the fiber composite as discrete layers—even when the material is fabricated by stacking pre-pregs and hot-pressing—is at best an approximation. This prompts the search for an alternative model, which is also simpler to use. Here in Part II, we present a model for an unlayered beam which is weak in shear; the resulting theory turns out to be rather simple to apply. In addition, the unlayered shear-weak model leads to results which are quantitatively similar to those of the layered beam, provided the number of layers is large.

2. DESCRIPTION OF MODEL AND ANALYSIS

Our model for a shear-weak beam assumes that the maximum sustainable shear stress on axes parallel and normal to the beam axis is τ_p; normal stresses along the same set of axes are not limited. This corresponds to classical perfect plasticity with infinite anisotropy (Hill, 1948). While we will refer below to a "plastic zone", in general the terminology "plastic" will be avoided, instead, we refer to the beam as "shear-weak".

The implications of these assumptions may be readily appreciated. Let the beam be subjected to distributed or concentrated transverse forces or moments. At a cross-section x, these loads give rise to bending moment $M(x)$ and shear force $V(x)$. Within the elementary engineering theory of elastic beams having rectangular cross-section, the stress resultants correspond to the following well-known distributions of normal stress $\sigma(y)$ and shear stress $\tau(y)$:

$$\sigma(y) = \frac{M}{I} y, \tag{1a}$$

$$\tau(y) = \frac{3V}{2A}\left(1 - 4\frac{y^2}{H^2}\right), \tag{1b}$$

where H is the thickness of the beam, b is width, $I = bH^3/12$ and $A = bH$.

The maximum shear stress in any cross-section x is at the center $y = 0$, and has the value $\tau_{max} = 3V/2A$. Provided $\tau_{max} < \tau_p$, or $V < V_p$ where V_p is defined by $2bH\tau_p/3$, the distributions (1) are valid for the beam with limited shear stress resistance. Once V exceeds V_p, the distributions change; the shear stress is equal to τ_p over the "plastic zone", which is described by $-H_p/2 < y < H_p/2$.

Now, imagine the shear strength τ_p has been reached in cross-sections of the beam which extend over some length $x_1 < x < x_2$. This defines a plastic region characterized by $H_p(x)$, where $H_p(x_1) = H_p(x_2) = 0$. Since the shear stress is constant and equal to τ_p in this region, the equilibrium equation

$$\frac{\partial \tau}{\partial y} = -\frac{\partial \sigma}{\partial x} \tag{2}$$

implies that the normal stress σ is independent of x, though possibly dependent on y. To deduce the normal stress, note that with a shear force present, the bending moment must vary with x through the plastic region. Since the normal stress is connected with the bending moment, only a spatially constant normal stress would seem to be plausible. Moreover, zero net axial force would seem to imply that $\sigma = 0$ in the whole plastic region. While the above argument lends plausibility to the contention that the normal stress vanishes in the plastic region, specifying $\sigma = 0$ and $\tau = \tau_p$ may be viewed as defining the constitutive law in the plastic regime. Since one of our purposes is to put forth a simplified theory which leads to results similar to those associated with discretely layered beams that suffer interlayer slippage, justification for our theory will be in its comparison with the discrete case.

Now, the additional assumption of axial strain continuity at $|y| = H_p/2$ implies that the axial strain and stress must also be zero on the elastic side of the boundary. (As is typical with beam theory, we are not concerned with the other normal component of stress.) Within the elastic portion of the cross-section ($H_p/2 < |y| < H/2$), the usual assumptions of elastic beam theory still hold: σ varies linearly with y, and τ varies parabolically with y, vanishing at the surface $|y| = H/2$. The stress distributions which balance the stress resultants in the cross-section, that is,

$$\iint_A \sigma(y) y \, dA = M, \tag{3a}$$

$$\iint_A \tau(y) \, dA = V, \tag{3b}$$

are given by

$$\sigma(y) = \frac{MH^3}{(2H+H_p)(H-H_p)^2 I}(2y \pm H_p), \tag{4a}$$

$$\tau(y) = C_v\left[\frac{H(H-2H_p)}{4} \mp H_p y - y^2\right], \tag{4b}$$

where

$$C_v = \frac{12V}{b(2H+H_p)(H-H_p)^2}.$$

The boundary of the plastic region is given by

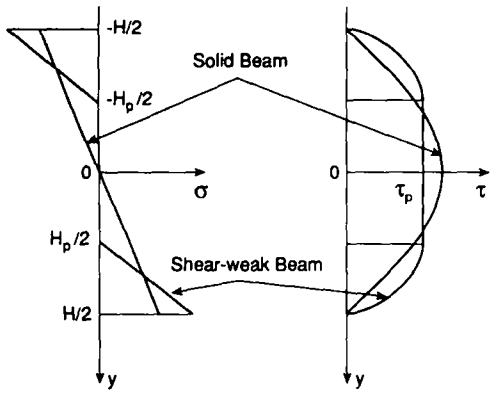

Fig. 1. Comparison of stresses in solid and shear-weak beams.

$$H_p = \left(3\frac{V}{V_{max}} - 2\right)H, \tag{5}$$

where V_{max}, given by $bH\tau_p$, is the maximum permissible shear force, at which the plastic zone engulfs the entire cross-section. In eqns (4), the upper sign refers to the region $-H/2 < y < -H_p/2$, and the lower sign to the region $H_p/2 < y < H/2$.

Note that the stress distributions at a cross-section are uniquely related to the values of M and V at that cross-section. By contrast, the stresses in the discretely layered beam are, in general, dependent on the entire distribution of $M(x)$ $a$and $V(x)$. For a case of $V > V_p$, the stress distributions in a solid beam and the shear-weak beam are compared in Fig. 1.

The crucial element of this theory for shear-weak beams is the change in the normal stress distribution that is associated with reaching the limiting shear resistance. Consider, in particular, the normal stress at the beam surface $|y| = H/2$, which is given by

$$s_{max} = \mp \frac{MH}{9I}\left(1 - \frac{V}{V_{max}}\right)^{-1}\left(\frac{V}{V_{max}}\right)^{-1}. \tag{6}$$

This tensile stress s_{max}, normalized by the tensile stress σ^s_{max} at the surface of an elastic beam under the same bending moment, is plotted in Fig. 2 as a function of V/V_{max}. Note that the stresses agree until $V/V_{max} = 2/3$ (at which point $V = V_p$). Thereafter, the maximum stress in the shear-weak beam exceeds that of the elastic beam, becoming unbounded as $V/V_{max} \to 1$.

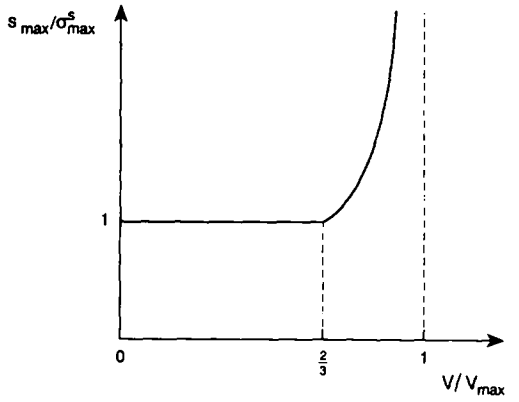

Fig. 2. Dimensionless maximum tensile stress as a function of shear force.

One can also compute the curvature in the shear-weak beam by considering the strain variation with y in the elastic portion of the beam; it is given by

$$w'' = -\frac{2M}{27EI}\left(1-\frac{V}{V_{\max}}\right)^{-2}\left(\frac{V}{V_{\max}}\right)^{-1}. \tag{7}$$

Since the curvature in a wholly elastic beam is given by

$$w'' = -\frac{M}{EI}, \tag{8}$$

one can immediately see a similar dependence of the curvature on the $V/V_{\max}$.

Unlayered shear-weak beams can be completely analysed using eqns (3), (5) and (7). In statically indeterminate situations the stress resultants and the deflections (the integral of the curvature) must be found simultaneously.

3. COMPARISON WITH DISCRETELY LAYERED BEAMS

In this section we present a quantitative comparison between a discretely layered beam investigated in Part I and the shear-weak beam introduced in Part II. To begin, we compare "plastic zone" sizes as a function of the shear force; for the shear-weak beam, H_p is related to V by eqn (5). In a discretely layered beam, slip initiates somewhere along the central interface; as the load increases, slip initiates at successive interfaces. Thus, in the discretely layered beam, there is not a "plastic zone" whose size is a continuous function of loading. Nevertheless, for purposes of comparison, it is possible to define a plastic zone thickness H_p^* for a discretely layered beam. If, at a given cross-section, the shear stress has reached the level τ_p at n^*+1 interfaces, then H_p^* is defined as n^*h, which is the distance between the outermost interfaces which have begun to slip.

The associated shear force can be determined as follows. Let $V^*(n^*)$ be the shear force at which slip first initiates at the outer two of the n^*+1 interfaces; for $V < V^*(n^*)$, there is slip at n^*-1 or fewer inferfaces. The equation relating H_p^* and $V^*(n^*)$ is derived by asserting the condition that τ equals τ_p at the outer two interfaces, e.g. $\tau(-n^*h/2) = \tau_p$ at the compressive side of the beam. In fact, with the procedure described in Part I, the distribution $\tau(y)$ in the portion of the beam which includes $y = -n^*h/2$ can be computed by noting that the region $-H/2 \leqslant y \leqslant -(n^*-2)h/2$ has no internal slip; that is, it is a single beamlet, at least up to the instant $V = V^*(n^*)$. From $\tau(-H/2) = 0$, $\tau[-(n^*-2)h/2] = \tau_p$, and V_j given by eqn (9) in Part I, one finds the distribution to be

$$\tau(y) = \tau_p\left[n(nf_1+f_2)+\frac{2n}{H}f_2 y-\left(\frac{2n}{H}\right)^2 f_1 y^2\right], \tag{9}$$

where

$$f_1 = 3\frac{2n\dfrac{V}{V_{\max}}-[n(1+\chi^*)-2]}{[n(1-\chi^*)+2]^3+4(n\chi^*-2)},$$

$$f_2 = \frac{1}{n(1-\chi^*)+2}-[n(1+\chi^*)-2]f_1,$$

and the dimensionless thickness $\chi^* = H_p^*/H$ takes on the values $\chi^* = n^*/n$, $(n^* = 2, 4, \ldots, n-2)$.

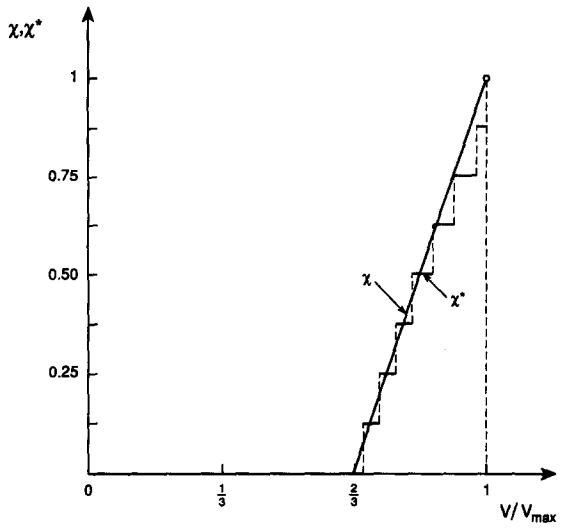

Fig. 3. Comparison of plastic zone size χ^* in discretely layered beam ($n = 16$) and χ in shear-weak beam.

The condition

$$\tau(-H_p^*/2) = \tau_p, \tag{10}$$

then provides the following third-order algebraic equation relating χ^* and $V^*(n^*)$:

$$n^2\chi^{*3} - 3n\left(n\frac{V}{V_{max}} + 1\right)\chi^{*2} + \left[6(n+1)n\frac{V}{V_{max}} - 3n^2 + 2\right]\chi^* - n\left[3(n+2)\frac{V}{V_{max}} - 2n - 3\right] = 0. \tag{11}$$

When χ^* takes on the discrete values n^*/n, ($n^* = 2, 4, \ldots, n-2$), eqn (11) defines the values of V/V_{max} which are $V^*(n^*)/V_{max}$.

For the particular case of 16 layers, the normalized plastic zones χ and χ^* are compared in Fig. 3 as a function of the shear force V/V_{max}. To quantify the discrepancy between the shear forces associated with a fixed normalized plastic zone size $\chi = \chi^*$, we employ an error measure e_1 defined by

$$e_1 = \frac{V - V^*(n^*)}{V^*(n^*)}. \tag{12}$$

Table 1 shows the error e_1 for three plastic zone sizes and for several beams composed of different number of layers n. On the whole the errors are rather small; furthermore, the general trend is for the error to decrease as n increases.

In fact, one can obtain the limiting behavior directly: as $n \to \infty$, eqn (11) becomes

Table 1. Discrepancy between model predictions of shear force to reach various plastic zone sizes

	Percentage discrepancy between slipping-layers model and unlayered shear-weak model $e_1 \times 100\%$				Unlayered shear-weak model
χ, χ^*	$n = 8$	$n = 16$	$n = 32$	$n = 64$	V/V_{max}
0.25	3.878	2.319	1.215	0.671	0.750
0.50	1.709	1.462	0.970	0.483	0.833
0.75	−4.280	−0.758	0.219	0.328	0.917

$$\chi^{*3}-3\frac{V}{V_{\max}}\chi^{*2}+3\left(2\frac{V}{V_{\max}}-1\right)\chi^{*}-\left(3\frac{V}{V_{\max}}-2\right)=0. \tag{13}$$

Equation (13) has three roots:

$$\chi_1^*=3\frac{V}{V_{\max}}-2,\quad \chi_2^*=\chi_3^*=1, \tag{14}$$

the first of which coincides with the dimensionless plastic zone in the shear-weak beam, as given by eqn (5). In this limit, χ^* is defined for all values of $V/V_{\max}$.

Consider now the distributions of tensile stress. In the shear-weak beam, the axial stress in the plastic zone is identically zero, and then increases linearly from 0 at $y=\mp H_p/2$ to a maximum at the beam surface $y=\mp H/2$. By contrast, the discretely layered beam has an axial stress distribution, as shown in Fig. 4. Of interest are the maximum stresses in the interior layers and the maximum stress at the beam surface in the discretely layered beam. Specifically, we consider the stresses in the discretely layered beam subjected to three-point bending with no overhang. (The effect of the overhang was treated in Part I.)

The extreme value of the tensile (and compressive) stress in the layers bounded by slipping interfaces for $i=(n-n^*)/2+1,\ldots,n^*$, normalized by the tensile stress $\sigma^s_{\max}$ at the surface in a solid beam, is given by

$$\frac{s_{i\text{extr}}}{\sigma^s_{\max}}=\mp\frac{4n}{4\chi^*+n^2(1-\chi^*)^3}\left[1-(1+\chi^*)\frac{3}{4p}\right], \tag{15}$$

where $p=3P/4bH\tau_p$ is the non-dimensional loading.

The tensile stress at the surface of the discretely layered beam, normalized by the tensile stress $\sigma^s_{\max}$ at the same point in a solid beam, is given by

$$\frac{s_{n\max}}{\sigma^s_{\max}}=\frac{2n^2(1-\chi^*)}{4\chi^*+n^2(1-\chi^*)^3}\left[1-(1+\chi^*)\frac{3}{4p}\right]+\frac{1}{1-\chi^*}\frac{1}{2p}. \tag{16}$$

As before, we first show the results for the specific case of a 16 layer beam. Plotted in

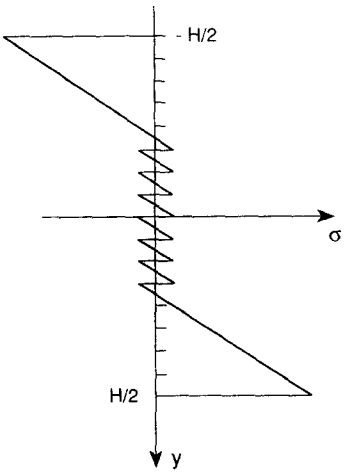

Fig. 4. Schematic of axial stress distribution in discretely layered beam.

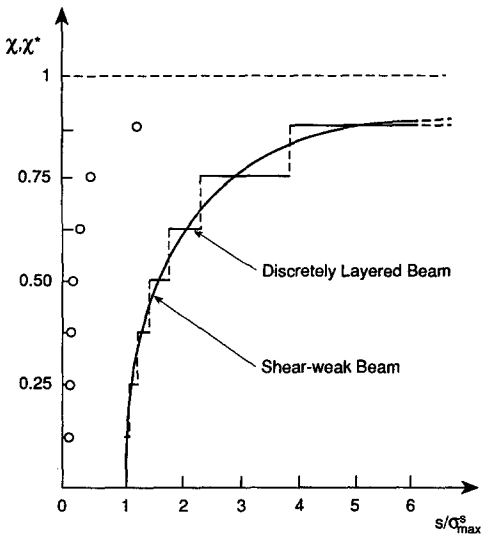

Fig. 5. Comparison of surface axial stress in discretely layered beam ($N = 16$) and shear-weak beam. ⊙ denotes maximum stress in interior layers bounded by slipping interfaces.

Fig. 5 are the stresses given in eqn (15) and eqn (16), as a function of the size of the dimensionless plastic zone. Consider first the stress at the surface of the beam. When slip first initiates at a new interface, the stress is less in the discretely layered beam than it is in the shear-weak beam. Just before slip initiates at the next surface, the stress is greater in the discretely layered beam than it is in the shear-weak beam. Care must be taken in making this comparison, however, as the stress is being compared for different levels of applied load. This point is addressed again below.

Also shown in Fig. 5 (as the discrete data points) are the maximum stresses in the internal slipping layers, again normalized by the maximum stress in a solid elastic beam. These stresses are relatively small for small plastic zone sizes, and increase with the plastic zone size. They should be compared with the zero stresses in the plastic zone of the shear-weak beam, as well as with the maximum stress at the surface of the discretely layered beam. One can see that the interior stresses are quite small by comparison with the surface stress, at least for small plastic zone sizes.

A second error measure, e_2, is now introduced in order to quantify the discrepancy between the maximum stress in the discretely layered beam and in the shear-weak beam:

$$e_2 = \frac{S_{\max} - S_{n\max}}{S_{n\max}}. \tag{17}$$

The percentage error is plotted in Fig. 6 as a function of χ^* for several values of n. Not only does the error decrease as n increases, but, for a fixed n, the error is less for smaller plastic zones χ^* than for larger plastic zones χ^*.

Limiting values of eqn (15) and eqn (16) for $n \to \infty$ are readily obtained. The maximum stress in the slipping layers approaches zero as $O(1/n)$ provided χ^* is not 1. One can see directly from eqn (15) that the rate at which the stress decreases diminishes as χ^* increases. On the other hand, for a large number of layers, the stress at the free surface behaves like

$$\lim_{n\to\infty} \frac{S_{n\max}}{\sigma^s_{\max}} = \frac{2}{(1-\chi^*)^2}\left[1-(1+\chi^*)\frac{3}{4p}\right] + \frac{1}{1-\chi^*}\frac{1}{2p}. \tag{18}$$

This is equivalent to the maximum stress in the shear-weak beam derived from eqn (6)

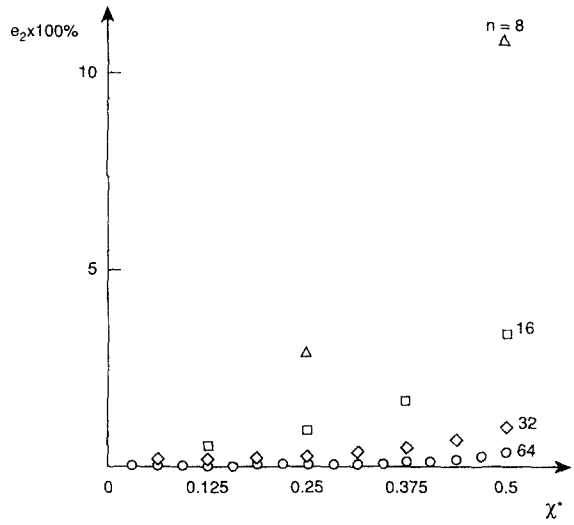

Fig. 6. Discrepancy between discretely layered and shear-weak beam predictions of surface axial stress.

$$\frac{s_{\max}}{\sigma^{s}_{\max}} = \frac{1}{(3-2p)p}, \tag{19}$$

provided that χ^* in eqn (18) has the value given by (14) appropriate to three-point bending, i.e. $\chi^* = 2(p-1)$.

A slightly different perspective on the maximum bending stress is gained from Fig. 7 in which the normalized tensile stress at the free surface is plotted as a function of the dimensionless load p. Now it can be seen that when the surface stress in the discretely layered beam (finite n) is compared with the shear-weak beam ($n \to \infty$) for the same value of load, the shear-weak beam gives a higher estimate of the stress enhancement. Furthermore, the variation with n is greater for larger p (corresponding to χ^* closer to 1) than for smaller p. In this connection, the significant difference between the discretely layered beam and the shear-weak beam should be noted. There is no limit to the load which can be applied to the discretely layered beam. Taking Fig. 4 to its logical progression, one can see that, as the load becomes large, each layer of finite thickness h takes up $1/n$ of the

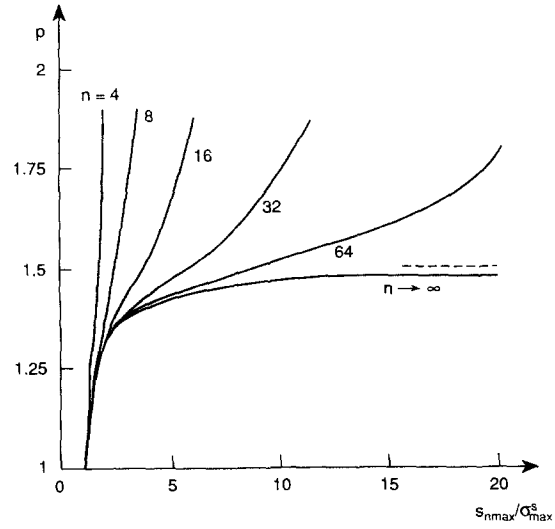

Fig. 7. Dependence of maximum axial stress on dimensionless load p for various number of layers; $n \to \infty$ corresponds to shear-weak model.

bending moment, just as in the motivating example of the deck of cards. The shear-weak beam, on the other hand, can withstand only so much load. Comparisons between the two models will be poor, therefore, when the shear force exceeds V_{max}. It is interesting, however, that V_{max} is not too dissimilar from the load at which slip begins in the outermost interfaces of the discretely layered beam. Thus, provided V is not too close to V_{max}, using the theory for the unlayered shear-weak beam appears to be reasonable.

4. DISCUSSION

One significant feature of the theory for unlayered shear-weak beams is that the greatest deviations from standard beam theory arise when the bending moment and the shear force are high in the same locations, i.e. under simultaneous shear and bending. The combination is more detrimental than either loading by itself; this is roughly akin to the more familiar case of metal plasticity. Say a metal sustains a shear stress which is less than the shear yield stress and a tensile stress which is less than the tensile yield stress. Depending on the yield criterion under combined stresses, this metal could very well still yield.

One can, in fact, set up a failure surface where the axes are shear force and bending moment. Let the tensile failure stress of the material be σ_{max}; under pure bending, the moment that produces this stress at the surface of the beam is M_{max}, which is given by $bH^2\sigma_{max}/6$. With τ_p being the shear strength, $V_{max} = bH\tau_p$ is the shear force at which shear failure occurs. In Fig. 8, we plot the locus of points $(V/V_{max}, M/M_{max})$ at which failure occurs. The interesting portion of the failure locus is the curved part which is described by

$$\frac{M}{M_{max}} = \mp\frac{9}{2}\left(1-\frac{V}{V_{max}}\right)\frac{V}{V_{max}}, \tag{20}$$

for $2V_{max}/3 < V < V_{max}$. In this portion of the locus, failure occurs because the axial stress equals σ_{max} at the surface. However, the bending moment which produces this stress at the surface is less than M_{max} because the limited shear resistance has enhanced the axial stresses at the surface.

In the previous section, it was shown that the stresses in an unlayered shear-weak beam are quantitatively similar to the stresses in a layered beam, provided there are sufficient numbers of layers, and provided the load is below that which causes slip on all interfaces of the layered beam. In the study of the layered beam in three-point bending (Part I), one essential parameter that was not explored was L/H—the length-to-height aspect ratio. The influence of this parameter on the response in three-point bending is explored here using the theory for unlayered shear-weak beams.

Let P_{max} denote the load at which the maximum bending stress in a perfect beam equals the tensile strength σ_{max}, i.e. $P_{max} = 2bH^2\sigma_{max}/3L$. If P denotes the load at which the maximum bending stress in the shear-weak beam equals σ_{max}, then one can find

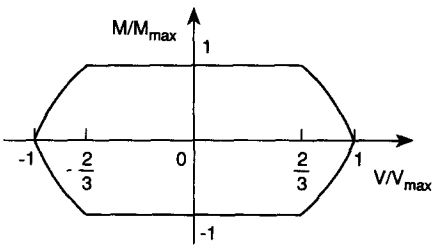

Fig. 8. Failure surface in space of dimensionless bending moment and shear force.

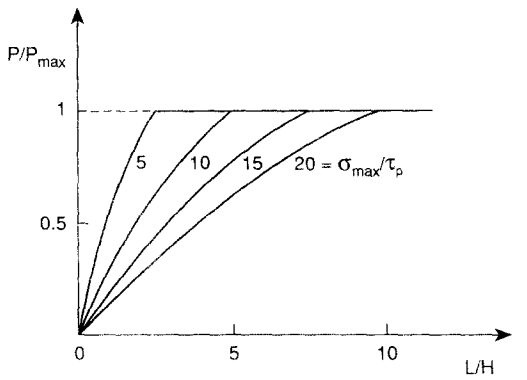

Fig. 9. Failure load in three-point bending as a function of beam aspect ratio.

$$\frac{P}{P_{\max}} \begin{cases} \left[3-2\frac{L}{H}\left(\frac{\sigma_{\max}}{\tau_p}\right)^{-1}\right]\frac{L}{H}\left(\frac{\sigma_{\max}}{\tau_p}\right)^{-1} & \text{for } 0 \leqslant \frac{L}{H} \leqslant \left(\frac{L}{H}\right)^*, \\ 1 & \text{for } \frac{L}{H} > \left(\frac{L}{H}\right)^*, \end{cases} \tag{21}$$

where $(L/H)^* = \sigma_{\max}/2\tau_p$ denotes the highest aspect ratio at which the strength is reduced, for a given ratio of $\sigma_{\max}/\tau_p$. In Fig. 9 $P/P_{\max}$ is plotted as a function of L/H.

It can be seen that shorter beams are apparently weaker, and that the effect of the aspect ratio becomes more pronounced as $\sigma_{\max}/\tau_p$ increases. This dependence of the failure load appears to be observed by Prewo and Nardone (1986) in their investigation of carbon-fiber reinforced glasses. They found that the apparent flexural strength $\sigma_{\text{flex}} = 3LP_{\max}/2bH^2$, increased as the aspect ratio increased. A detailed quantitative comparison between these experimental results and the present model is being simultaneously reported (Steif and Trojnacki, 1992).

Finally, it is important to note that the impact of weakness in shear depends strongly on the loading. Three-point bending is a loading which one can expect to produce substantially different stresses in a shear-weak beam and in a solid beam. This is because the bending moment is maximum at a point of high shear force. Consider, by contrast, a simply-supported beam under a uniformly distributed applied transverse load. The bending moment is maximum in the middle of the beam where the shear force is zero; the shear force is maximum at the supports, where the bending moment is zero. The effect of shear-weakness will clearly be minimal under this loading.

Acknowledgements—P.S.S. was supported by Air Force Office of Scientific Research grant 890548 and A.T. was supported by Department of Energy grant DE-FG02-89ER45404. Assistance provided by General Electric Aircraft Engines and by the Department of Mechanical Engineering, Carnegie Mellon University is also gratefully acknowledged.

REFERENCES

Hill, R. (1948). A theory of the yielding and plastic flow of anisotropic metals. *Proc. R. Soc. London* **A193**, 281–297.

Prewo, K. M. and Nardone, V. C. (1986). Carbon fiber reinforced glass matrix composites for space based applications. Report No. R86-917161-1, United Technologies Research Center.

Steif, P. S. and Trojnacki, A. (1992). Bend strength versus tensile strength of fiber-reinforced ceramics. *J. Amer. Cer. Soc.* (to be published).